Microwave-Assisted Synthesis and Chemical Modulation of MOF-74(Ni)

by
Abdulrahman N. Aldossary

A PROJECT

submitted to

Oregon State University

University Honors College

in partial fulfillment of
the requirements for the
degree of

Honors Baccalaureate of Science in Chemical Engineering (Honors Associate)

Presented May 26, 2015
Commencement June 2015

AN ABSTRACT OF THE THESIS OF

Abdulrahman Aldossary for the degree of Honors Baccalaureate of Science in Chemical Engineering presented on May 26, 2015. Title: Microwave-Assisted Synthesis and Chemical Modulation of MOF-74(Ni).

Abstract approved:

_____

Gregory S. Herman

Metal-organic frameworks (MOFs) are crystalline porous material distinguished for high free empty volume and pore tunability. MOF-74(Ni) was previously shown to be effective in adsorbing carbon dioxide, methane, and hydrogen. Microwave-assisted synthesis of MOF-74(Ni) was shown to lower reaction time from days to hours. In this thesis, experimental conditions of batch microwave-assisted synthesis of MOF-74(Ni) were investigated. Crystallinity was investigated using powder X-ray diffraction and Raman spectroscopy. Chemical modulation effect was also investigated, in which a ligand is added to precursor solution to compete with linkers for coordination with metal cations. The highest relative crystallinity was achieved when reaction was run for 2 hours at 90 °C. Crystallinity was further increased when one-tenth equivalent of benzoic acid was added to precursor solutions and titrated with sodium hydroxide.

Key Words: MOF-74(Ni), CPO-27-Ni, metal-organic frameworks (MOFs), batch microwave-assisted synthesis, chemical modulation

Corresponding e-mail address: aldossary.abdulrhaman@gmail.com

Microwave-Assisted Synthesis and Chemical Modulation of MOF-74(Ni)

by
Abdulrahman N. Aldossary

A PROJECT

submitted to

Oregon State University

University Honors College

in partial fulfillment of
the requirements for the
degree of

Honors Baccalaureate of Science in Chemical Engineering (Honors Associate)

Presented May 26, 2015
Commencement June 2015

Honors Baccalaureate of Science in Chemical Engineering project of Abdulrahman Aldossary presented on May 26, 2015.

APPROVED:

Gregory S. Herman, Mentor, representing Chemical, Biological, and Environmental Engineering Department

Chih-Hung Chang, Committee Member, representing Chemical, Biological, and Environmental Engineering Department

Ki-Joong Kim, Committee Member, representing Chemical, Biological, and Environmental Engineering Department

Toni Doolen, Dean, University Honors College

I understand that my project will become part of the permanent collection of Oregon State University, University Honors College. My signature below authorizes release of my project to any reader upon request.

Abdulrahman Aldossary, Author

Acknowledgements:

The author acknowledges Gustavo Albuquerque for lab assistance and help with characterization, Prof. Herman for mentorship and guidance, and Prof. Chih-Hung Chang and Dr. Ki-Joong Kim for serving as committee members. The author also acknowledges Profs. Yokochi and Nason for access to UV-Vis and DLS systems, respectively.

I would like to also thank my family and friends for their support during my school years.

Fiat Lux

Table of Contents:

List of Figures:

List of Tables:

Microwave-Assisted Synthesis and Chemical Modulation of MOF-74(Ni)

Chapter 1: Introduction:

1.1 Thesis overview:

The adsorption of MOF-74(Ni) is tunable by synthesis parameters including reaction temperature, time and chemical modulators in the precursor solution. Effects of reaction conditions on crystallinity through varying temperature, time, and chemical modulators were studied to optimize adsorption capacity.

1.2 MOF Overview:

Metal-organic frameworks (MOFs) are a new class of crystalline, porous materials that has been extensively investigated in the last several decades due to their large surface area, free empty volume, and pore size tunability [1, 2]. MOFs typically consist of metal ions and organic linkers. They are distinguished for having rigid secondary building units (SBUs) containing metal cations with open sites surrounded by linkers. SBUs are substitutable yielding materials with different properties and functionalities associated with the open metal cation sites [2]. Those open metal sites allow physisorption of gases opening horizons for future applications for MOFs, including gas storage [3, 4, 5, 6, 7, 8, 9], gas separation [3, 10, 11], catalysis [3, 12, 13], drug delivery [14, 15], and sensors [3, 16, 17].

The thesis focus is on MOF-74(Ni) which is known for its relative stability in the presence of water. It also has high adsorption capacities for carbon dioxide [7, 18, 19], methane [7], hydrogen [6, 20], hydrogen sulfide [8], and water [18]. It was shown to effectively separate carbon dioxide preferentially over methane and nitrogen [7, 21], hydrogen [22], and water [18]. It is also known to have one of the highest enthalpies of adsorption for hydrogen compared to other MOFs [1, 20]. This makes MOF-74(Ni) interesting for industrial applications that involve gas separation, carbon sequestration, and hydrogen storage to meet Department of Energy targets [5].

1.3 MOF Synthesis:

MOF-74(Ni) are composed of 2,5-dihydroxyterephthalic acid (DOBDC) and nickel ions creating a honeycomb structure conventionally referred to as MOF-74. Nickel ions, provided by nickel acetate, form an octahedral structure bounded firmly by carboxylic acid's functionalized benzene rings derived from DOBDC as can be shown in Figure 1. MOF-74 pores have diameters about ~11 Å [6].

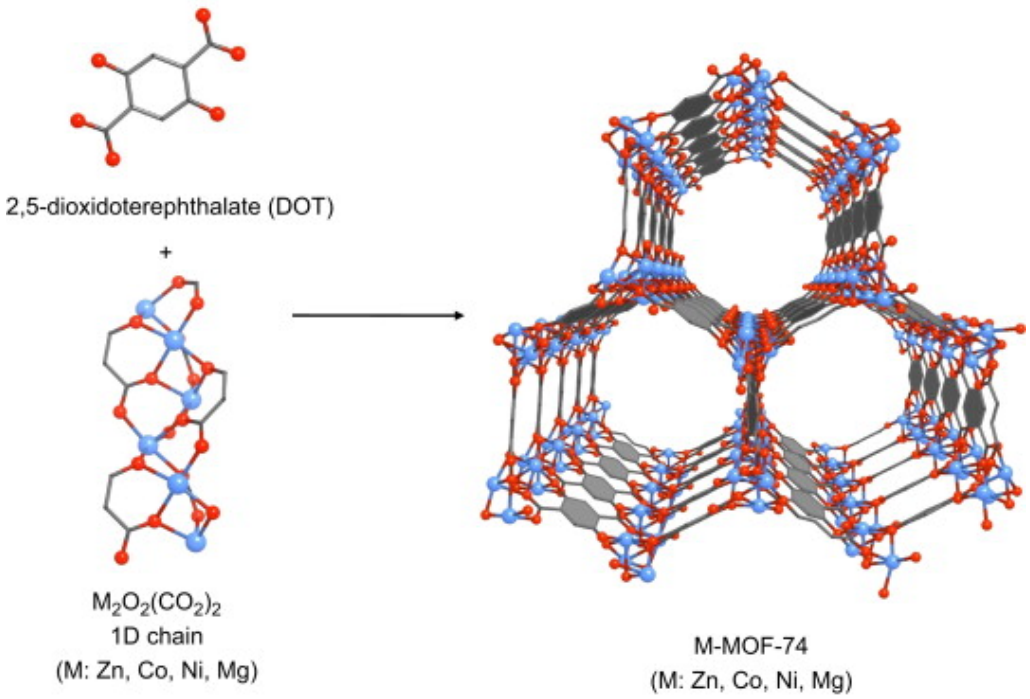

Figure 1. "Synthesis of MOF-74 metal analogs." Reproduced with permission from Ref. [8].

MOF synthesis begins with nucleation when reagents start reacting [23]. Nucleation is the limiting-rate step in most MOFs. Classical theory of nucleation assumes hard spheres crystallizing, more like metallic structures, and less like MOF structure. According to classical theory of nucleation, nucleation is exponentially dependent on temperature, to lower entropy of the system and drive crystal formation [24]. It is also directly proportional to concentration as more nucleation sites are available. For thermodynamic purposes, nucleation requires high enthalpy to rule over the entropy loss of crystallization.

Nucleation is a metastable state that is stabilized by growth when crystals extend. For crystalline structures, activation energy of growth has to be considerably lower than that of nucleation, creating more ordered structures rather than amorphous phases. The disparity in activation energies of nucleation and growth is a key concept in synthesis of crystalline material. The growth and nucleation mechanisms provide relatively more crystalline structures with lower reaction temperature. In contrary, reaction occurs too fast at higher temperatures, and reactive species will not find enough thermodynamic energy to crystallize and tend to have more defects. On the other hand, lower reaction temperature produces less crystalline material due to lack of required thermodynamic energy. Heating crystalline particles for extended time allows them to adjust to less disordered structures to minimize the dangling bonds. However, longer time in heated conditions is economically infeasible.

Monocrystalline material surface has high-energy dangling bonds on the surface while disordered material will have dangling bond and defects throughout. Monocrystalline structures are more likely to combine together while polycrystalline particles agglomerate without chemically bonding due to the topography of those structures. A prominent phenomenon known as Ostwald ripening occurs when small particles dissolve to create bigger ones. This is driven by the interest of minimizing the total energy since smaller particles tend to be less energetically stable.

Chemical modulation is an established method to lower reaction rate [25, 26, 27]. It was also found to increase crystallinity, surface area and adsorption capacity [26]. Chemical modulators are added to precursor solution in which added ligands compete with linkers in coordination and hinder both nucleation and growth. The chemical modulators investigated herein are benzoic acid and acetic acid. Both modulators are acidic ($K_{A,benzoic\ acid}$ = 6.46x10^{-5}, $K_{A,acetic\ acid}$ = 1.76x10^{-5}) [28] and change precursor solution's pH significantly. Titrating acidic modulators is important to restore reagents reactivity to uniform levels.

1.4 Microwave-Assisted Synthesis:

Conventionally, MOF-74-Ni is made by solvothermal synthesis in which precursors are placed in oven for few days. Although known for its fine temperature and pressure control, it lacks uniform temperature profile causing non-uniform nucleation and growth mechanisms. Microwave synthesis of MOF-74-Ni was found to dramatically reduce reaction time from days to hours compared to conventional heating [21, 29, 30, 31, 32]. Irradiation absorption increases with increase in number of charge carriers and polar molecules that interact with microwaves. Microwave heating provides fine control over nucleation and growth synthesis steps by inducing volumetric heating and direct interaction with reagents. This makes synthesized particles' sizes more monodisperse [30]. A popular controversy in the field is about complementary effects from microwave interfering with reaction mechanism. Such interference was shown to be unlikely, and uniform heating stands solely for the observable difference [30].

Chapter 2: Methods:

2.1 Materials:

For each reaction, 0.597 g of $NiAc_2 \cdot 4H_2O$ were dissolved in 20 mL water, and 0.238 g of 2,5-dihydroxyterephthalic acid (DOBDC) was dissolved 20 ml dimethylformamide (DMF). Solutions were mixed and stirred for five minutes creating the reactant mixture (30 mM $NiAc_2$ and 15 mM DOBDC). Some experiments included additions of 0.1, 1 and 3 equivalents of benzoic acid (0.015, 0.147, and

0.440 g) and acetic acid (0.007, 0.069, and 0.206 mL) separately. Sodium hydroxide was then used to titrate acidic modulators using a pH meter before they were added to precursor solution. Chemicals were used as purchased. DMF (99.8%) was obtained from EMD, $NiAc_2 \cdot 4H_2O$ (>98%) was obtained from Alfa Aesar, DOBDC (>98%) was obtained from TCI America, benzoic acid pellets (>99.5%) was obtained from J. T. Baker, acetic acid (>99.7%) was obtained from Macron and sodium hydroxide pellets (>98%) were obtained from Macron. Two vessels were filled with 14 mL each and loaded to CEM MARS Synthesis microwave as shown in Figure 2 with various temperature and time reaction conditions.

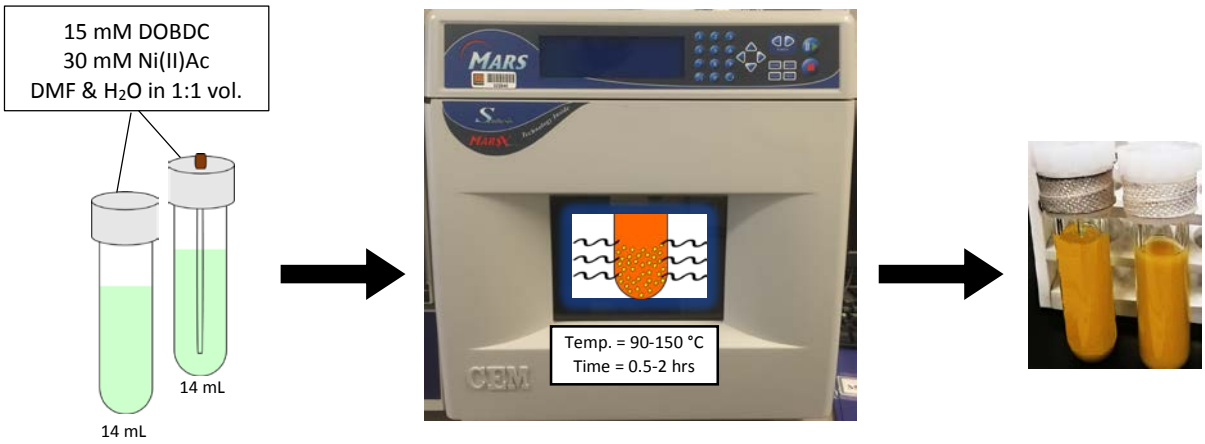

Figure 2. Work flow diagram of batch microwave-assisted synthesis of MOF-74(Ni).

2.2 Synthesis Approach:

First, MOF-74(Ni) was synthesized at various temperatures and times. Reaction time and temperature were matrix-swept between 30 and 120 min. and 90, 120, and 150 °C. Those conditions have been shown to successfully produce MOF-74(Ni) [21, 29]. One reaction involved a temperature ramp to 150 °C followed by 2-hour hold time at 90 °C. This reaction condition should induce vast particle nucleation followed by growth region to control crystallinity as shown in Figure 3. The objective was to investigate the effects of temperature and time on reaction products.

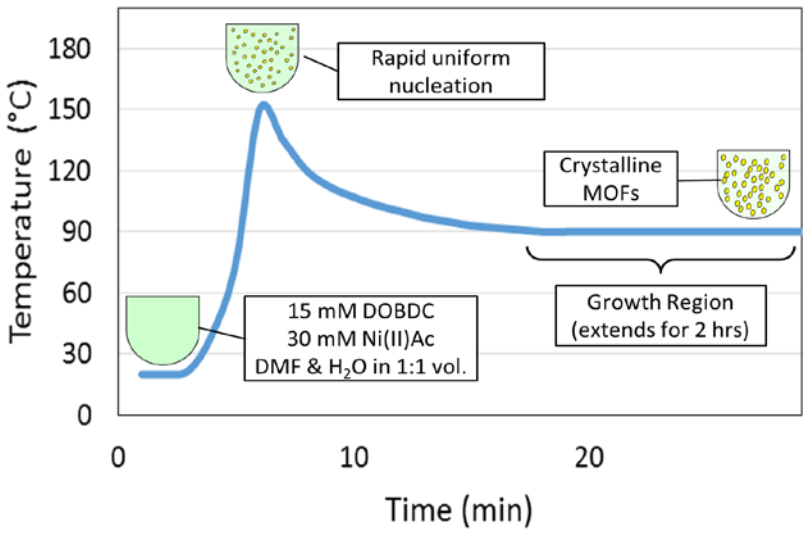

Figure 3. Schematic showing the temperature ramp with the expected outcomes on reaction mechanism.

Second, MOF-74(Ni) synthesis was modulated by adding 0.1, 1, and 3 equivalents of benzoic acid and acetic acid separately. Sodium hydroxide was then used to titrate acidic modulators before they were added to precursor solution. All reactions experienced a temperature ramp to 150 °C followed by 2-hour hold time at 90 °C. Temperature ramp was modified to include a hold time of ~5 sec. at 150 °C to account for variation in ions concentration which results in different energy absorption and temperature profile. The objective was to investigate the effects of chemical modulation at different concentrations on crystallinity and reaction rate.

Dispersed MOFs solution is centrifuged after each reaction. Solution was used in UV-Vis spectroscopy to find conversion as will be discussed later. Solid MOFs were transferred to ethanol solution, sonicated, and then centrifuged again to remove DMF. Activation consisted of keeping MOFs in methanol solution for 3 days, with replacing methanol every 24 hours to further expel DMF from pores. It was then vacuum-dried at 80 °C, with additional 30 min. of 120 °C.

2.3 Characterization:

Ultraviolet-visible spectrophotometry (UV-Vis) was used to evaluate reaction conversion. A spectrophotometer sends radiation through a tubular cell and measures absorbed light at various wavelengths. Wavelength used was 627 nm as can be seen in Figure 4 which corresponds to absorption peak for DOBDC since it appears yellow. The adjacent peak is associated with nickel ions since they appear green. Beer's law was used to find product solution concentration, and its condition of low concentration was met since reactant concentration is 30 mM Ni^{2+}. Measurements were obtained from an AvaSpec-3648 spectrometer.

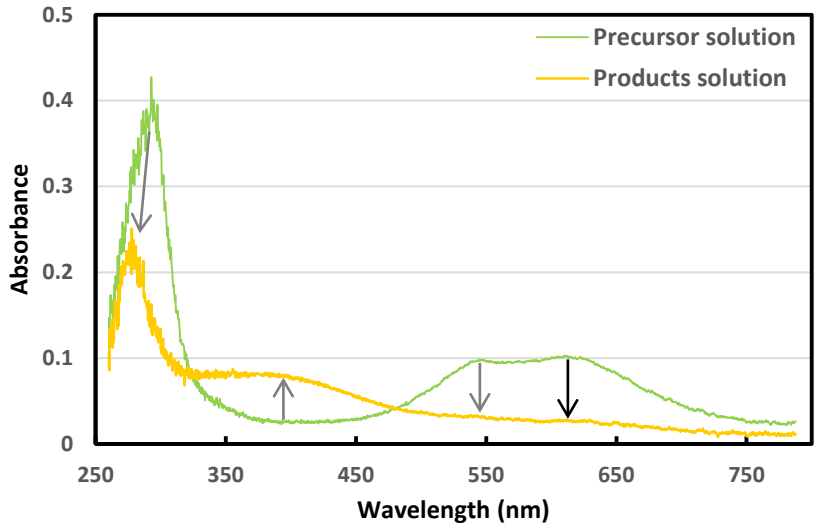

Figure 4. UV-Vis absorbance spectrum of precursor and products solutions is shown. Peaks shift as reaction progresses as indicated by the arrows. Bold, black arrow indicates the absorbance shift at the used wavelength of 627 nm.

Dynamic light scattering (DLS) was used to estimate effective particle diameter and its distribution. DLS device shines light through a sample that gets scattered by particles. Particles scattering is related to Brownian motion. Smaller particles diffuse faster and scattered light intensity will change faster according to Stokes-Einstein equation in relation to their diameters. Diameters presented represent those of spheres that exhibit similar diffusion property. Polydispersity was calculated as square of ratio between standard deviation and mean. Samples were prepared using ultrasonic waves to disaggregate the particles for 30 minutes. They then were left to settle shortly before measurements were obtained using Brookhaven Zeta Potential analyzer.

Powder X-ray diffraction (PXRD) was used to get a quantifiable measure of MOFs crystallinity based on the narrowness of diffraction angles. The machine shines X-rays at a sample and measures diffracted light at different angles based on atomic spacing according to Bragg's Law. X-ray light absorbed by electrons is reemitted with the same frequency but delayed based on twice the atomic spacing traveled to adjacent atom by light. More polycrystalline material tends to have random distribution of angles around the angle of the related atomic spacing. Single-crystal material, in contrast, will have one narrow peak. PXRD was performed at room temperature using a Rigaku Ultima IV diffractometer (Cu-Kα = 0.1542 nm). Measured angles of 2θ ranged from 5 to 50°.

Raman spectroscopy was used as a redundant crystallinity measurement and to verify presence of MOF-74(Ni) when different modulators are added. The device shines laser light at a sample while measuring

inelastically scattered light due to Raman active molecular vibrations or phonons of the crystal structure. It is typically used as a fingerprint of a material to identify chemical structures. For the purpose of this paper, it was used to quantify crystallinity such that narrower peaks indicate more crystalline structure, higher uniformity and less defects. Product powder was ground, mixed with ethanol, and dried on a silicon substrate. Measurements were obtained using Horiba-Jobin Yvon HR-800 Raman spectrometer with a 532-nm incident laser source.

Chapter 3: Results and Discussion:

3.1 Temperature-Time Effects:

First, reactions were run at various temperatures and times. Conversions calculated using spectrophotometry is shown in Table 1 with particle size distribution. Diameters and polydispersity were obtained through the DLS technique. Diameters shown correspond to single particles due to prior sonication. PXRD measurements are shown in Figure 5 to compare crystallinity.

Table 1. Conversion and particle size distribution for MOF-74(Ni) synthesized at various conditions are shown. Reaction conversion is directly proportional to reaction temperature and time. Shorter reaction times tend to have narrower particle size distribution, whereas longer reaction times' particle size distribution is heavily affected by temperature.

Temperature	Time	Conversion (%)	Average Effective Diameter (nm)	Polydispersity
150 °C	120 min.	93.4	962	0.032
150 °C	30 min.	84.9	324	0.005
120 °C	120 min.	83.8	932	0.043
120 °C	30 min.	81.0	375	0.005
90 °C*	120 min.	89.0	517	0.142
90 °C	120 min.	69.9	806	0.192
90 °C	30 min.	52.0	668	0.005

*Temperature ramp to 150 °C briefly was induced in this reaction.

Higher temperatures and longer reaction times yield higher conversion. Polydispersity increases as reaction progresses due to continuous nucleation of particles. This is demonstrated clearly in the 2-hour 90 °C reaction where lower probability of nucleating particles continues longer creating polydisperse material (pdi = 0.192). Particle size increases as reaction progresses due to growth and Ostwald ripening. Given long reaction time, higher temperatures produce bigger particles due to abundance of thermal energy to stimulate growth and nucleation (962 nm). For shorter times, the 90 °C shows the biggest

particle due to low nucleation rate allowing growth to be the predominant mechanism. Note that due to the same reason, the conversion was found to be fairly low (X = 52.0). Conversion increased considerably when temperature ramp was introduced making nucleation the predominant regime (X = 89.0). The immense increase in nucleation rate consumed most of reagent which reduced particles sizes significantly.

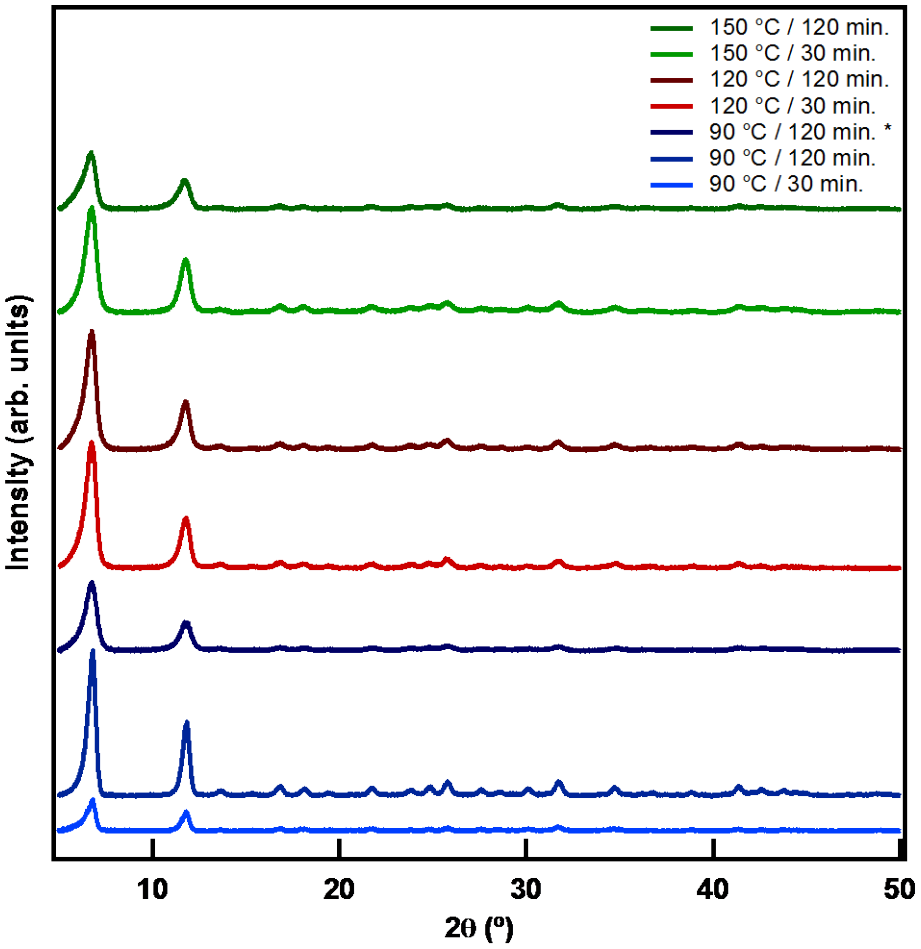

Figure 5. MOF-74(Ni) synthesized at various conditions was analyzed using powder X-ray diffraction technique. Narrower peaks correspond to more crystalline particles. Peaks are located at consistent positions signifying the presence of MOF-74(Ni). *Temperature ramp to 150 °C briefly was induced in this reaction.

Narrower peaks correspond to less defects and higher relative crystallinity. Increasing reaction time increases crystallinity for 90 °C, has negligible effect on 120 °C, and reduces crystallinity at 150 °C. At 90 °C, premature particles need more time to adjust into crystalline structures. More time drives them to the growth regime, adjusting slowly to more crystalline material. At 150 °C, particles are in nucleation regime are small (324 nm) and have moderately high crystallinity. As reaction progresses, Ostwald

ripening becomes the predominant mechanism for growth, and particles become bigger (962 nm) and their relative crystallinity drops consequently.

3.2 Modulators Effect:

Second, reagents are held at 90 °C for 2 hours after a hold of ~5-sec. at 150 °C. Chemical modulators were titrated and added to precursor solution. Chemical modulators compete with linkers in coordination and reduce reaction rate. Benzoic acid and acetic acid ligands coordinate with nickel cations stifling reaction. Conversions calculated using spectrophotometry is shown in Table 2 with particle size distribution. Diameters and polydispersity were obtained through the DLS technique. Diameters shown correspond to single particles due to prior sonication. PXRD measurements are shown in Figure 6 to compare crystallinity. Raman spectroscopy measurements are shown in Figure 7 to compare crystallinity.

Table 2. Conversion and particle size distribution of MOF-74(Ni) synthesized with chemical modulators are shown. Reaction conversion reduces with adding more chemical modulators.

Modulation	Conversion (%)	Average Effective Diameter (nm)	Polydispersity
3.0 Eq. benzoic acid	68.0		
1.0 Eq. benzoic acid	85.9		
0.1 Eq. benzoic acid	92.5	789	0.054
3.0 Eq. acetic acid	71.8		
1.0 Eq. acetic acid	94.7		
0.1 Eq. acetic acid	96.7	427	0.078
No modulators	97.7	313	0.116

Benzoic acid was found to reduce conversion more than acetic acid, so higher crystallinity for particles synthesized with benzoic acid is expected. Diameters increase with modulators due to slowdown of reaction.

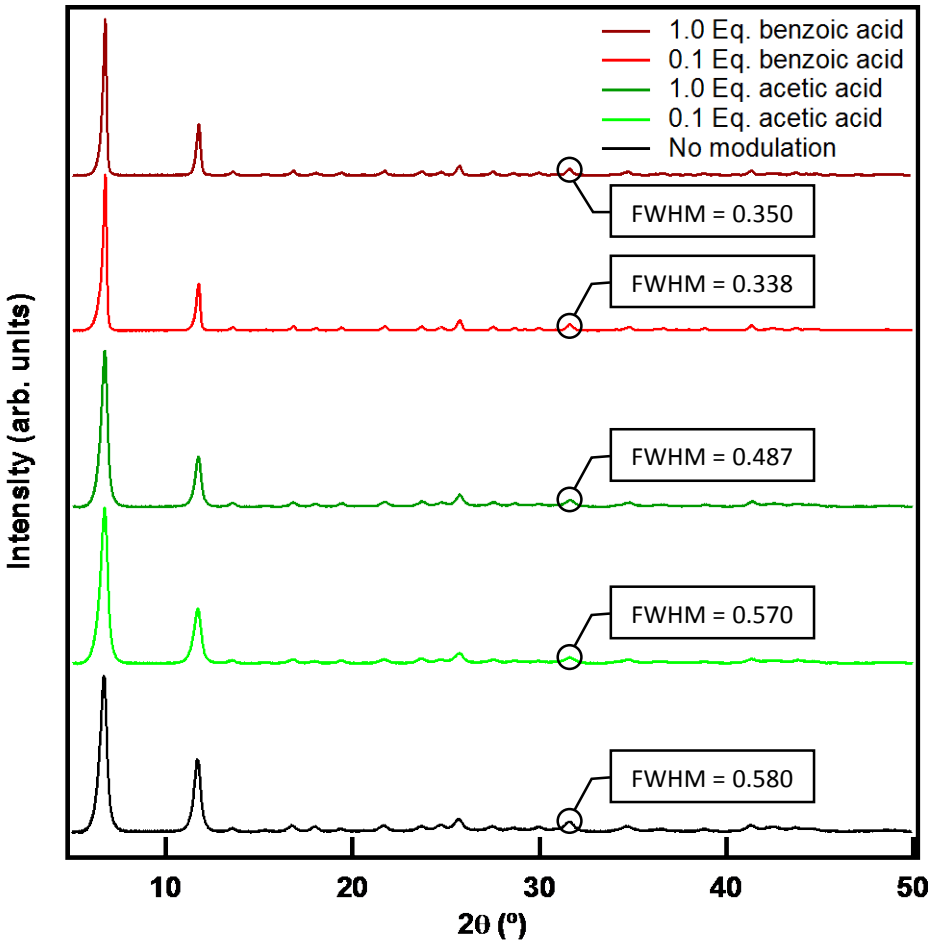

Figure 6. MOF-74(Ni) synthesized at various chemical modulation was analyzed using powder X-ray diffraction technique. FWHM (full width at half maximum) is shown for the peak at 2θ = 31.7°. Peaks are located at consistent positions signifying the presence of MOF-74(Ni) even when modulators are added.

Highest intensities were observed at 2θ of 6.8° and 11.8° which match literature values [29]. Chemical modulation at 3 eq. showed no peaks at all for benzoic acid and acetic acid, indicating amorphous material. Due to insignificant visual difference, narrowness was quantified by comparing the FWHM (full width at half maximum) for each peak at 2θ = 31.7° as shown in Figure 6. Addition of benzoic acid increases crystallinity more than an equivalent amount of acetic acid. This can be due to greater coordination between benzoate ligands and the metallic cations relative to that of acetate. When benzoic acid is added in 1 eq., product MOF becomes more disordered. This is due to overly slowing down the reaction kinetics but not the available thermal energy causing the material to be more disordered. Another explanation could be defects resulted from benzoate ligands coordinating in MOF-74 structure. Acetate competition for coordination was lower relatively that increasing acetic acid just slowed the reaction without reaching adversely too slow reaction rate.

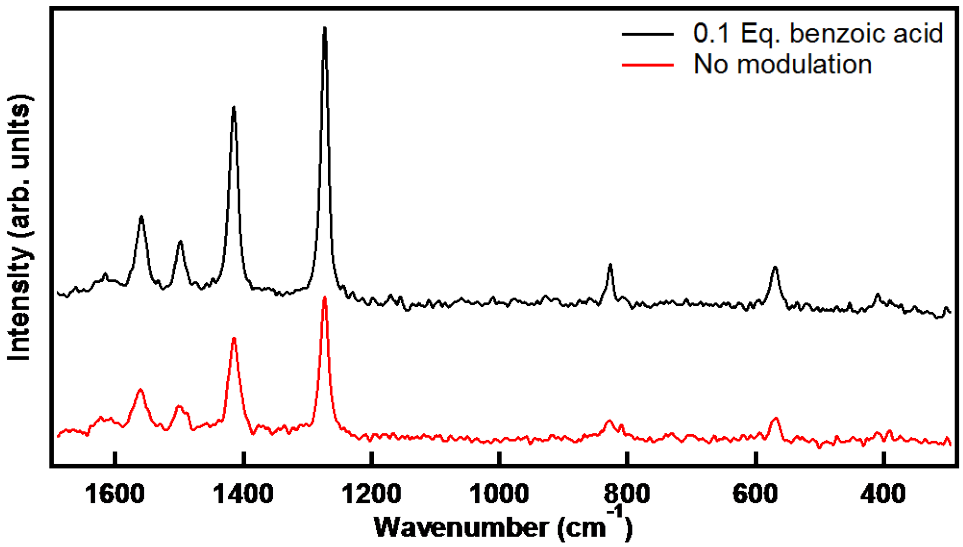

Figure 7. Raman peaks are shown for MOF-74(Ni) synthesized with and without chemical modulation. Peaks were narrower and more intense when benzoic acid was added to MOF-74(Ni) precursors in agreement with powder X-ray diffraction results. Results indicate no change in chemical structure as peaks were observed at the same wavelengths.

Addition of 0.1 eq. benzoic acid shows no change in chemical structure. This suggests that benzoate ligands are competing for coordination, but do not take a part in synthesis. Raman peaks match literature value for MOF-74(Ni) [33].

Chapter 4: Conclusion

4.1 Summary:

MOF-74(Ni) was successfully synthesized in a batch microwave reactor with reduced reaction times. Operating conditions were optimized to increase yield with reasonable crystallinity. The temperature profile used indicates that nucleation and growth can be probabilistically separated. Adding chemical modulator to precursor solution was found to significantly increase crystallinity when 0.1 eq. of benzoic acid was added.

4.2 Future Work:

More DLS measurements need to be made to further study reaction mechanism when chemical modulators are added. Raman spectroscopy measurement of 1 eq. benzoic acid can be used to corroborate the hypothesis of benzoate presence in MOF-74 structure. Finally, nitrogen physisorption measurements need to be made to verify whether the change in relative crystallinity will result in improved adsorption performance.

References

[1] H. Furukawa, K. E. Cordova, M. O'Keeffe and O. Yaghi, *Science,* p. 1230444, 2013.

[2] O. M. Yaghi, M. O'Keeffe, N. W. Ockwig, H. K. Chae, M. Eddaoudi and J. Kim, *Nature,* vol. 432, pp. 705-714, 2003.

[3] R. J. Kuppler, D. J. Timmons, Q.-R. Fang, J.-R. Li, T. A. Makal, M. D. Young, D. Yuan, D. Zhao, W. Zhuang and H.-C. Zhou, *Coordination Chemistry Reviews,* vol. 253, pp. 3042-3066, 2009.

[4] H. W. Langmi, J. Ren, B. North, M. Mathe and D. Bessarabov, *Electrochimica Acta,* vol. 128, pp. 368-392, 2014.

[5] D. J. Durbin and C. Malardier-Jugroot, *International Journal of Hydrogen Energy,* vol. 38, pp. 14595-14617, 2013.

[6] P. D. C. Dietzel, B. Panella, M. Hirscher, R. Bloma and H. Fjellva°g, "Hydrogen adsorption in a nickel based coordination polymer with open," *The Royal Society of Chemistry,* p. 959–961, 2006.

[7] P. D. C. Dietzel, V. Besikiotis and R. Blom, *Journal of Materials Chemistry,* vol. 19, pp. 7362-7370, 2009.

[8] T. G. Glover, G. W. Peterson, B. J. Schindler, D. Britt and O. Yaghi, *Chemical Engineering Science,* vol. 66, pp. 163-170, 2011.

[9] S. Chavan, F. Bonino, L. Valenzano, B. Civalleri, C. Lamberti, N. Acerbi, J. H. Cavka, M. Leistner and S. Bordiga, vol. 117, pp. 15615-15622, J. Phys. Chem..

[10] J.-R. Li, J. Sculley and H.-C. Zhou, *Chemical Reviews,* vol. 112, pp. 869-932, 2012.

[11] Z. R. Herm, E. D. Bloch and J. R. Long, *Chemistry of Materials,* vol. 26, pp. 323-338, 2014.

[12] J. Lee, O. K. Farha, J. Roberts, K. A. Scheidt, S. T. Nguyen and J. T. Hupp, *Chemical Society Reviews,* vol. 38, p. 1450–1459, 2009.

[13] P. Mahata, G. Madras and S. Natarajan, *J. Phys. Chem. B,* vol. 110, pp. 13759-13768, 2006.

[14] R. C. Huxford, J. D. Rocca and W. Lin, *Current Opinion in Chemical Biology,* vol. 14, p. 262–268, 2010.

[15] P. Horcajada, T. Chalati, C. Serre, B. Gillet, C. Sebrie, T. Baati, J. F. Eubank, D. Heurtaux, P. Clayette, C. Kreuz, J.-S. Chang, Y. K. Hwang, V. Marsaud, P.-N. Bories, L. Cynober and S. Gil, *Nature Materials,* vol. 9, p. 172–178, 2010.

[16] B. Chen, Y. Yang, F. Zapata, G. Lin, G. Qian and E. B. Lobkovsky, *Adv. Mater.,* vol. 19, pp. 1693-1696, 2007.

[17] M. Albrecht, M. Lutz, A. L. Spek and G. v. Koten, *Nature,* vol. 406, pp. 970-974, 2000.

[18] J. Liu, P. K. Thallapally, B. P. McGrail, D. R. Brown and J. Liu, *Chem. Soc. Rev.,* vol. 41, pp. 2308-2322, 2012.

[19] A. O. Yazaydın, R. Q. Snurr, T.-H. Park, K. Koh, J. Liu, M. D. LeVan, A. I. Benin, P. Jakubczak, M. Lanuza, D. B. Galloway, J. J. Low and R. R. Willis, *J. Am. Chem. Soc.,* vol. 131, pp. 18198-18199, 2009.

[20] J. G. Vitillo, L. Regli, S. Chavan, G. Ricchiardi, G. Spoto, P. D. C. Dietzel, S. Bordiga and A. Zecchina, *J. Am. Chem. Soc.,* vol. 130, pp. 8386-8396, 2008.

[21] X. Wu, Z. Bao, B. Yuan, J. Wang, Y. Sun, H. Luo and S. Deng, *Microporous and Mesoporous Materials,* vol. 180, pp. 114-122, 2013.

[22] D.-J. Lee, Q. Li, H. Kim and K. Lee, *Microporous and Mesoporous Materials,* vol. 163, pp. 169-177, 2012.

[23] O. Shekhah, H. Wang, D. Zacher, R. A. Fischer and C. Woll, *Angew. Chem. Int. Ed.,* vol. 48, pp. 5038-5041, 2009.

[24] R. P. Sear, *J. Phys.: Condens. Matter,* vol. 19, p. 28, 2007.

[25] M.-H. Pham, G.-T. Vuong, F.-G. Fontaine and T.-O. Do, *Cryst. Growth Des.,* vol. 12, pp. 3091-3095, 2012.

[26] A. Schaate, P. Roy, A. Godt, J. Lippke and F. Waltz, *Chem. Eur. J.,* vol. 17, p. 6643–6651, 2011.

[27] A. Umemura, S. Diring, S. Furukawa, H. Uehara, T. Tsuruoka and S. Kitagawa, *J. Am. Chem. Soc.,* vol. 133, pp. 15506-15513, 2011.

[28] S. S. Zumdahl and S. A. Zumdahl, Chemistry, 6th Edition, 2002.

[29] J. S. Lee, S. B. Halligudi, N. H. Jang, D. W. Hwang, J.-S. Chang and Y. K. Hwang, *Bull. Korean Chem. Soc.,* vol. 31, pp. 1489-1495, 2010.

[30] G. A. Tompsett, W. C. Conner and K. S. Yngvesson, *ChemPhysChem,* vol. 7, pp. 296-319, 2006.

[31] E. Haque and S. H. Jhung, *Chemical Engineering Journal,* vol. 173, p. 866– 872, 2011.

[32] C. Dey, T. Kundu, B. P. Biswal, A. Mallick and R. Banerjee, *Acta Crystallographica,* vol. 70, pp. 3-10, 2014.

[33] L. Valenzano, J. Vitillo, S. Chavan, B. Civalleri, F. Bonino, S. Bordiga and C. Lamberti, *Catalysis Today,* vol. 182, pp. 67-79, 2012.